Possible Influence of Tropical Indian Ocean Sea Surface Temperature on the Proportion of Rapidly Intensifying Western North Pacific Tropical Cyclones during the Extended Boreal Summer

JUN GAO,[a,b] HAIKUN ZHAO,[c] PHILIP J. KLOTZBACH,[d] CHAO WANG,[a] GRACIELA B. RAGA,[e,f] AND SHAOHUA CHEN[a]

[a] *Key Laboratory of Meteorological Disaster of Ministry of Education, Nanjing University of Information Science and Technology, Nanjing, China;* [b] *Key Laboratory of South China Sea Meteorological Disaster Prevention and Mitigation of Hainan Province, Haikoum, China;* [c] *Key Laboratory of Meteorological Disaster, Ministry of Education/Joint International Research Laboratory of Climate and Environment Change/Collaborative Innovation Center on Forecast and Evaluation of Meteorological Disaster/Pacific Typhoon Research Center/Earth System Modeling Center, Nanjing University of Information Science and Technology, Nanjing, China;* [d] *Department of Atmospheric Science, Colorado State University, Fort Collins, Colorado;* [e] *Centro de Ciencias de la Atmósfera, Universidad Nacional Autónoma de Mexico, Mexico City, Mexico*

(Manuscript received 10 February 2020, in final form 20 July 2020)

ABSTRACT: This study examines the possible impact of tropical Indian Ocean (TIO) sea surface temperature anomalies (SSTAs) on the proportion of rapidly intensifying tropical cyclones (PRITC) over the western North Pacific (WNP) during the extended boreal summer (July–November). There is a robust interannual association ($r = 0.46$) between TIO SSTAs and WNP PRITC during 1979–2018. Composite analyses between years with warm and cold TIO SSTAs confirm a significant impact of TIO SSTA on WNP PRITC, with PRITC over the WNP basin being 50% during years with warm TIO SSTAs and 37% during years with cold TIO SSTAs. Tropical cyclone heat potential appears to be one of the most important factors in modulating the interannual change of PRITC over the WNP with a secondary role from midlevel moisture changes. Interannual changes in these large-scale factors respond to SSTA differences characterized by a tropics-wide warming, implying a possible global warming amplification on WNP PRITC. The possible footprint of global warming amplification of the TIO is deduced from 1) a significant correlation between TIO SSTAs and global mean SST (GMSST) and a significant linear increasing trend of GMSST and TIO SSTAs, and 2) an accompanying small difference of PRITC (~8%) between years with detrended warm and cold TIO SSTAs compared to the difference of PRITC (~13%) between years with nondetrended warm and cold TIO SSTAs. Global warming may contribute to increased TCHP, which is favorable for rapid intensification, but increased vertical wind shear is unfavorable for TC genesis, thus amplifying WNP PRITC.

KEYWORDS: Tropical cyclones; Climate variability; Interannual variability; Tropical variability

1. Introduction

Tropical cyclones (TCs) frequently cause large economic damage and loss of life to various coastal regions, mainly through the direct impact of TC-generated strong winds and heavy rainfall, as well as the indirect impact of TC-associated meteorological and geological disasters (Zhang et al. 2009, 2011; Mendelsohn et al. 2012; Peduzzi et al. 2012; England et al. 2014; Lin et al. 2014). About 27 TCs occur annually over the western North Pacific (WNP) basin, accounting for ~1/3 of the average annual global TC total (Chan 2005; Schreck et al. 2014). Over the past several decades, there has been a substantial improvement in the forecast skill of TC track prediction (Rappaport et al. 2009; DeMaria et al. 2014). Until recently, however, little progress in TC intensity prediction has been made, with the ability to predict rapid intensification (RI) still being problematic (Elsberry et al. 2007; Rappaport et al. 2009). Recently, Emanuel (2017) suggested that global warming may favor RI of hurricanes before striking land, consequently making hurricane intensity forecasts more difficult. It is, therefore, important to explore key factors affecting the rapid intensification of TCs (RITC) and the associated underlying physical mechanisms on various time scales.

Large-scale atmospheric and oceanic environmental conditions including weak vertical wind shear, high midlevel relative humidity, warm sea surface temperature (SST), large upper-ocean heat content (OHC), and weak interaction between TCs and the surrounding upper-level circulation are recognized to be favorable for the RITC process (Emanuel 1999; Kaplan and DeMaria 2003; Mainelli et al. 2008; Goni et al. 2009; Wang et al. 2015; Wang and Liu 2016; Fudeyasu et al. 2018). Among these environmental factors, the role of the oceanic environment (e.g., OHC) in the development of RITC appears to be more important than the atmospheric conditions. For example, Zhao et al. (2018a) found a significantly increased proportion of rapidly intensifying TCs (PRITC) over the WNP basin since 1998, mainly associated with a significant increase in local tropical cyclone heat potential (TCHP). Moreover, they indicated that the reduced TC genesis frequency over the WNP basin in more recent years is mainly associated with unfavorable atmospheric factors, including decreased low-level vorticity and increased vertical wind shear. Guo and Tan (2018) emphasized the importance of TCHP in RITCs over the WNP basin, associated with both short- and long-lived El Niño events. Moreover, there is substantial improvement in the accuracy of hurricane intensity forecasts in several statistical models over the tropical Atlantic when TCHP is considered as a predictor (Mainelli et al. 2008; Goni et al. 2009).

It has been well documented that both global and basin SST anomalies (SSTAs) can exert direct as well as remote impacts on changes in the large-scale environment affecting WNP TC activity

[f] ORCID: 0000-0002-4295-4991.

Corresponding author: Dr. Haikun Zhao, zhk2004y@gmail.com

DOI: 10.1175/JCLI-D-20-0087.1

(Du et al. 2011; Zhan et al. 2011a,b, 2014, 2018; Zhao et al. 2014; Huo et al. 2015; Cao et al. 2016; L. Wang et al. 2017). Several recent studies have shown that the tropical Indian Ocean (TIO) has a significant impact on WNP TC frequency through changes in the East Asian–WNP monsoon circulation and associated atmospheric factors (Du et al. 2011; Tao and Cheng 2012; Zhan et al. 2011a,b, 2014; Zhao et al. 2014). The TIO capacitor has been proposed as the prevailing mechanism by Xie et al. (2009) due to its ability to change the equatorial Kelvin wave structure and thus impact the Indo-Pacific summer climate. Currently, the TIO has experienced a large increase in SST amplitude and has undergone a pronounced warming trend far exceeding its natural historical variability (Hoerling et al. 2004; Du and Xie 2008; Roxy et al. 2014; Hu and Fedorov 2019). The TIO has generally been thought to track the rise of global mean sea surface temperature (GMSST) (Ihara et al. 2009; Zheng et al. 2013; Dong and Zhou 2014; Hu et al. 2018). As global warming has continued, there has been a significant change in both East Asian and in WNP climate (Luo et al. 2012; Hu et al. 2014; Hu and Bates 2018; Xie et al. 2009, 2016). During this time, there has been a significant increase in the association between ENSO and TIO SSTAs (Zheng et al. 2011; Tao et al. 2015; Zhao et al. 2018a).

On interannual time scales, prior studies have mainly focused on the changes of atmospheric factors affecting WNP TC frequency in response to change in TIO SSTAs (Zhan et al. 2011a,b, 2014, 2018; Zhao et al. 2015), while the impact of interannual variability of TIO SSTAs on TC intensity change, and especially on PRITCs over the WNP basin, has been relatively less studied. Kang and Elsner (2019) pointed out a possible amplified effect of global warming on the increase in RITC count and the decrease in overall TC counts, thus increasing PRITC over the WNP basin. With regard to the possible impact of global warming, two questions naturally arise regarding the interannual variability of TIO SSTAs and its impacts on WNP TCs:

1) What are the important environmental factors for PRITC over the WNP basin?
2) What is the relative role of global warming on the observed changes in PRITC over the WNP basin?

This study will focus on these two questions from an observational perspective.

The remainder of this study is arranged as follows. Section 2 describes the data and methodology used. Section 3 examines the interannual relationship between TIO SSTAs and TC activity including TC counts, RITC counts, and PRITC over the WNP basin. In section 4, the key factors affecting RITC counts and PRITC over the WNP basin are explored from the associated changes in the large-scale oceanic and atmospheric environment in response to the interannual variability in TIO SSTAs. Section 5 further investigates the possible impact of global warming on WNP PRITC through its association with the interannual variability of TIO SSTAs. Section 6 gives a brief summary and discussion.

2. Data and methodology

a. Data

The TC data for the period 1979–2018 are obtained from the Joint Typhoon Warning Center (JTWC) best track dataset (Chu et al. 2002). This dataset includes TC location as denoted by latitude and longitude, maximum sustained surface winds, and minimum sea level pressure (since 2001 for most TCs) at a 6-h interval. All TCs during the peak season from July to November (JASON) with a maximum sustained wind speed equal to or greater than 34 kt ($\sim$17 m s^{-1}) (i.e., at least tropical storm intensity) are considered in this study.

Monthly atmospheric fields (e.g., air temperature, wind, relative humidity, and specific humidity) are obtained from the National Centers for Environmental Prediction–Department of Energy (NCEP–DOE) AMIP-II Reanalysis (Kanamitsu et al. 2002), with a 2.5° × 2.5° latitude and longitude resolution and 17 vertical pressure levels extending from 1000 to 10 hPa. Monthly SST is obtained from the National Oceanic and Atmospheric Administration (NOAA) Extended Reconstruction SST version 5 (ERSSTv5), which provides global and spatially complete SST data with a horizontal resolution of 2° × 2° (Huang et al. 2017).

b. Definition of RITC and calculation of TCHP

RITC is identified in this study as in previous studies (Wang and Zhou 2008; Zhao et al. 2018a) and must satisfy the following three criteria: 1) at least a 5-kt (1 kt ≈ 0.51 m s^{-1}) increase of TC intensity in the first 6 h, 2) at least a 10-kt increase of TC intensity in the first 12 h, and 3) at least a 30-kt increase of TC intensity in 24 h. The threshold of intensity change [i.e., 30 kt (24 h)$^{-1}$] has also been widely employed to define a RITC event since it generally represents the $\sim$95th percentile of 24-h intensity changes for WNP TCs (Shu et al. 2012). The PRITC is defined to be the proportion of rapidly intensifying tropical cyclones to the total number of tropical cyclones (e.g., RITC counts/TC counts) in this study. Thus PRITC is a measure of the likelihood of a TC to undergo rapid intensification.

Previous studies have noted the importance of TCHP on TC rapid intensification (Leipper and Volgenau 1972; DeMaria et al. 2005; Guo and Tan 2018; Zhao et al. 2018a). The TCHP is a measure of the integrated vertical temperature between the ocean surface and an estimate of the depth of the 26°C isotherm (Shay et al. 2000). The calculation of TCHP follows previous studies (Leipper 1967; Guo and Tan 2018; Zhao et al. 2018a) with the following expression:

$$\mathrm{TCHP} = C_p \rho \int_{D_{26}}^{0} [T(z) - 26]\, dz, \tag{1}$$

where C_p is the heat capacity of seawater at a constant pressure, which is taken as 4178 J kg^{-1} °C^{-1}; ρ is the density of seawater, which is taken as 1026 kg m^{-3} in the upper ocean; D_{26} is the depth of the 26°C isotherm; and $T(z)$ is the in situ temperature. The two variables, temperature and salinity, involved in the computation of TCHP are obtained from the Simple Ocean Data Assimilation 3 (SODA3; Carton et al. 2018), which is based on the Parallel Ocean Program ocean model with a 0.5° × 0.5° horizontal resolution and 50 vertical pressure levels. We do note the importance of warm eddies for rapid intensification of TCs (Shay et al. 2000; Goni and Trinanes 2003; Scharroo et al. 2005; Lin et al. 2005, 2008; Ma et al. 2017). The computation of TCHP using 2° × 2° SST data from NOAA ERSST-v5 in this study may smooth the impact of warm ocean eddies on TC rapid intensification. However, we also use higher-resolution 0.5° × 0.625° SST data from the Modern-Era Retrospective Analysis for Research and Applications, version

2 (MERRA-2; Gelaro et al. 2017) to compute TCHP and found almost identical results (figure not shown).

c. A diagnostic tool for the role of large-scale conditions in TC genesis

To explore the association between the large-scale environment and TC genesis, the genesis potential index (GPI) proposed by Emanuel and Nolan (2004) is adopted in this study. Studies have suggested that the GPI has a good representation of TC genesis over the WNP as well as other TC basins on intraseasonal to interdecadal time scales (Camargo et al. 2007, 2009; Hsu et al. 2014; Zhao et al. 2015, 2016, 2018b; Zhao and Wu 2018). The GPI is calculated using the following expression:

$$I_{\mathrm{GPI}} = |10^5\zeta|^{3/2} \times \left(\frac{H}{50}\right)^3 \times \left(\frac{V_{\mathrm{pot}}}{70}\right)^3 \times (1 + 0.1\mathrm{vws})^{-2}, \quad (2)$$

where ζ is the absolute vorticity at 850 hPa ($10^{-6}\,\mathrm{s}^{-1}$), H represents the relative humidity at 600 hPa (%), V_{pot} is the potential intensity (PI) ($\mathrm{m\,s}^{-1}$), and vws is the vertical wind shear between 850 and 200 hPa (200 hPa minus 850 hPa) ($\mathrm{m\,s}^{-1}$); V_{pot} represents the maximum TC potential intensity. Details on the physical mechanism underlying PI can be found in previous studies (Emanuel 1986, 1988, 2000). The PI is the theoretical upper bound on TC intensity under a given set of atmospheric and oceanic conditions and is calculated with the following expression (Emanuel 1995; Bister and Emanuel 2002):

$$V_{\mathrm{pot}}^2 = \frac{T_s}{T_0}\frac{C_k}{C_D}(\mathrm{CAPE}_{\mathrm{MS}} - \mathrm{CAPE}_M), \quad (3)$$

where T_S is SST (°C), T_o is the mean outflow temperature (°C), C_K is the exchange coefficient for enthalpy, and C_D is the drag coefficient. $\mathrm{CAPE}_{\mathrm{MS}}$ is the convective available potential energy (CAPE) for an air parcel brought to saturation at the radius of maximum winds; CAPE_M is the CAPE of a parcel brought to the radius of maximum winds without input of energy or moisture.

d. Statistical significance

The statistical significance of correlations and composite differences of TC variables and all environmental parameters in this study is performed with a one-tailed Student's *t* test. The differences and correlations are deemed to be statistically significant if the probability of the phenomenon being random is less than 1 in 20, resulting in a P value of $<5\%$ in this study, unless specifically stated otherwise.

3. Significant interannual association between TIO SSTAs and WNP PRITC

During the peak season (JASON), ~20.0 TCs and 8.6 RITCs are on average observed per year over the WNP basin, respectively, accounting for ~75% of the total of 26.5 TCs and 79% of the total of 10.9 RITCs over the WNP basin during 1979–2018. There is significant interannual variability in boreal summer TC frequency, RITC frequency, and PRITC over the WNP basin during the period from 1979–2018. There are, on average, ~20 TCs that occur during the peak TC season (JASON), with a standard deviation (STD) of 3.8 TCs. About 8.6 RITCs are annually observed, with a STD of 2.4 RITCs during 1979–2018. The annual-average PRITC rate is ~44%, with a STD of 12%. Furthermore, there are significant correlations between TC counts and RITC counts ($r = 0.47$), between RITC counts and PRITC ($r = 0.70$), and between PRITC and TC counts ($r = -0.29$). These significant correlations among these three parameters indicate that TC counts, RITC counts, and PRITC over the WNP basin share some common large-scale conditions. There are also some distinct factors that exist for differentiating TC counts, RITC counts, and PRITC over the WNP basin.

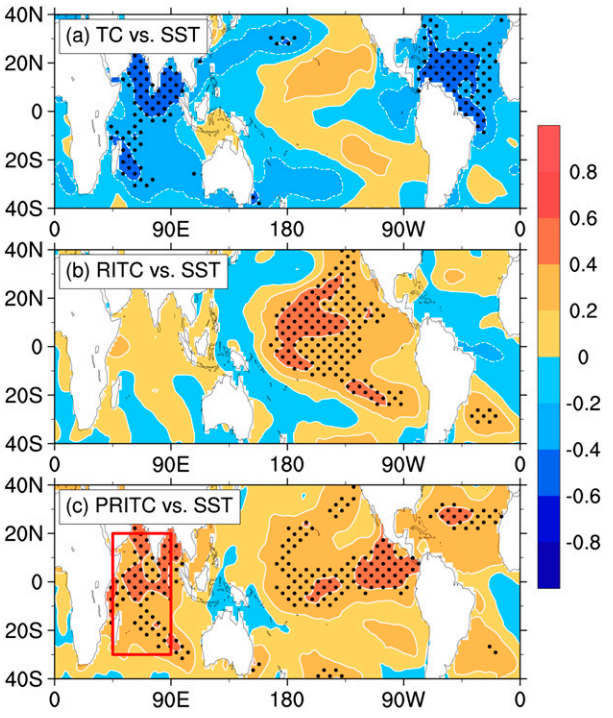

FIG. 1. Correlations of SST and (a) TC counts, (b) RITC counts, and (c) PRITC over the WNP basin during the peak TC season (July–November) from 1979 to 2018. The rectangular box (30°S–20°N, 45°–90°E) indicates the core TIO area that has significant correlations. The values with the black dots are statistically significant at a 95% confidence level.

Correlation maps between TC counts, RITC counts, and PRITC over the WNP basin and global SSTAs (Fig. 1) confirm that there are different factors and associated physical mechanisms driving each of these TC parameters. The TIO and tropical North Atlantic (TNA) correlate significantly with WNP TC count (Fig. 1a). This result agrees well with prior research noting the importance of changes in TIO and TNA SSTAs in modulating WNP TC frequency (Zhan et al. 2011a,b, 2014, 2018; Zhao et al. 2014; Huo et al. 2015; Cao et al. 2016; C. Wang et al. 2017). For example, Zhan et al. (2011a,b) pointed out that anomalous SSTAs in the tropical East Indian Ocean basin have had a strong impact on TC frequency over the WNP basin since the late 1970s. They hypothesized that this impact was primarily due to a warm (cold) equatorial Kelvin wave caused by warm (cold) EIO SSTAs decreasing (increasing) the surface

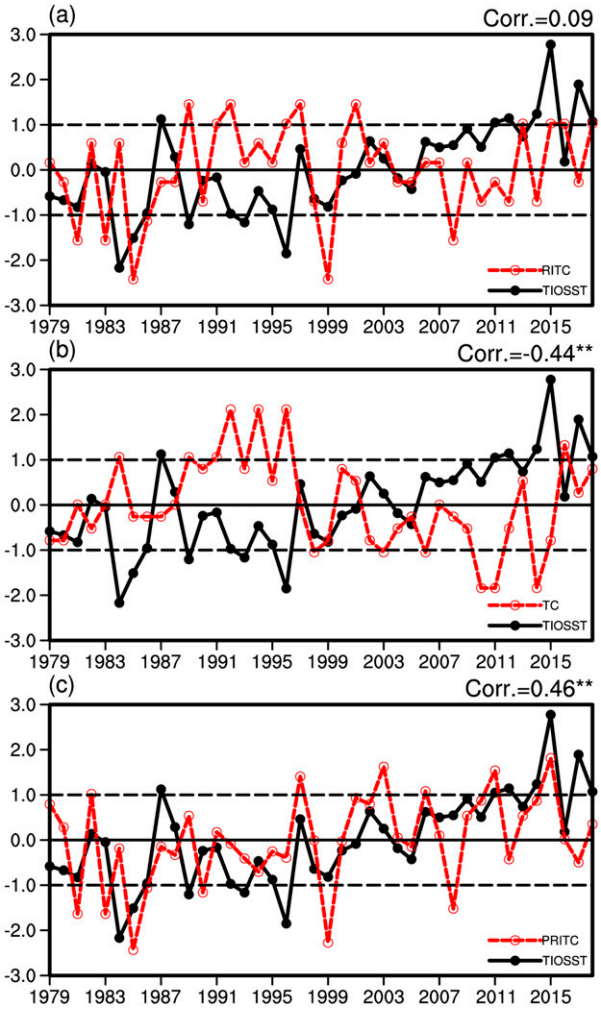

FIG. 2. Standardized time series of (a) annual WNP RITC counts (red) and the TIO SST index (black), (b) annual WNP TC counts (red) and the TIO SST index (black), and (c) annual WNP PRITC (red) and the TIO SST index (black). Correlation coefficients are shown in the upper-right corner of each panel, and values with two asterisks (**) indicate significance at a 95% confidence level.

pressure in the equatorial region. This then leads to anomalous anticyclonic (cyclonic) vorticity and divergence (convergence) over the WNP TC genesis region. Huo et al. (2015) found a strong influence of TNA SSTAs on TC frequency over the WNP basin through modulation of tropospheric midlevel humidity and large-scale vorticity. The correlation map between RITC frequency over the WNP basin and global SST displays an ENSO-like pattern (Fig. 1b), which agrees well with prior studies showing a strong modulation of ENSO on RITC location and occurrence over the WNP basin (Wang et al. 2015; Guo and Tan 2018; Shi et al. 2020). More importantly, a strong correlation with WNP PRITC is observed over the TIO, especially over the region bounded by 30°S–20°N, 45°–90°E (Fig. 1c).

We further examine the relationship between WNP TC activity and TIO SSTAs over the region bounded by 30°S–20°N, 45°–90°E (Fig. 2) during 1979–2018. TIO SSTAs have a weak correlation (~0.09) with WNP RITC counts (Fig. 2a), a significant correlation (~−0.44) with WNP TC counts (Fig. 2b), and a significant correlation (~0.46) with WNP PRITC (Fig. 2c). In summary, interannual changes in TIO SSTAs have a strong association with PRITC over the WNP basin. The associated physical mechanism behind this relationship has not been extensively studied. The close interannual relationship between TIO SSTAs and PRITC was noted in Zhao et al. (2018a). Zhao et al. (2018a) mainly focused on the Pacific climate regime shift and its relationship with the increase in PRITC over the WNP basin during recent decades. The associated underlying mechanism causing the strong association between TIO SSTAs and PRITC over the WNP basin was not further investigated in that study. We now focus on the important factors associated with interannual changes in TIO SSTs affecting PRITC over the WNP basin and explore associated plausible physical mechanisms.

4. Key factors affecting WNP PRITC associated with interannual changes in TIO SSTAs

To further clarify the effect of TIO SSTAs on the PRITC over the WNP basin, the years with strong warm (cold) TIO SSTAs are identified based upon the standardized annual TIO SSTAs over the region bounded by 30°S–20°N, 45°–90°E. We define strong warm (strong cold) TIO years as those where the SSTA is greater than (less than) or equal to 1 standard deviation (Fig. 2). We identify eight years with strong warm TIO SSTAs (i.e., 1987, 2009, 2011, 2012, 2014, 2015, 2017, and 2018) and six years with strong cold TIO SSTAs (i.e., 1984, 1985, 1986, 1989, 1992, and 1996). The following sections mainly focus on the composite analyses between these years with warm and cold TIO SSTAs. Note that the selection of these years with warm and cold TIO SSTAs is determined by the standardized annual time series of TIO SSTAs over the core region without removing the linear trend. The years with warm and cold TIO SSTAs without removing the linear trend are labeled as RAW-warm and RAW-cold TIO SSTAs. Later in this study we will present results in which the linear trend is removed, and the corresponding years will be identified as RWT-warm and RWT-cold TIO SSTAs.

During years with RAW-warm TIO SSTAs, there are ~17.8 TCs during the peak season over the WNP basin, which is significantly smaller than ~23.7 TCs during the peak season for RAW-cold TIO SSTAs. As shown in Fig. 3a, there is a decrease of TCs in the South China Sea (SCS), the Philippine Sea, and the eastern WNP basin during years with RAW-warm TIO SSTAs compared to that during years with RAW-cold TIO SSTAs. The change in TC counts may be caused by changes in atmospheric factors including suppressed low-level vorticity and increased vertical wind shear over the WNP basin in response to anomalously warm TIO SSTAs (Du et al. 2011; Xie et al. 2009, 2016; Wang et al. 2006) and associated divergence over the subtropical region that triggers suppressed convection over the WNP basin (Zhan et al. 2011a,b, 2014). In contrast, there is no significant difference in RITC counts (~0.4) over the WNP basin between years with RAW-warm and RAW-cold TIO SSTAs. There are ~8.6 RITCs over the WNP basin during years with RAW-warm TIO SSTAs and ~9.0 RITCs during years with RAW-cold TIO SSTAs annually, on average.

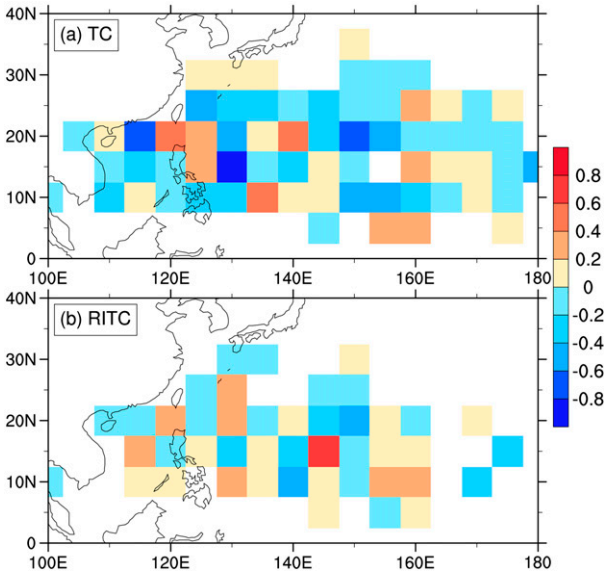

FIG. 3. Spatial distributions of the difference in (a) TC counts and (b) RITC counts in each 5° longitude × 5° latitude grid box over the WNP basin between years with warm and cold TIO SSTAs.

As shown in Fig. 3b, there is an increase in RITCs over the main development region of the WNP basin (7.5°–27.5°N, 110°–160°E) during years with RAW-warm TIO SSTAs relative to years with RAW-cold TIO SSTAs. Due to a significant difference in TC counts and little difference in RITC counts over the WNP basin, the annually averaged PRITC over the WNP is found to be higher (~50%) during years with RAW-warm TIO SSTAs and smaller (~37%) during years with RAW-cold TIO SSTAs. This difference in PRITC is significant at a 95% confidence level (Table 1).

We next examine composite differences of oceanic and atmospheric conditions (Fig. 4). As shown in Figs. 4a and 4b, there is an increase in vertical wind shear especially over the region bounded by 15°–25°N, 145°E–180° and a decrease in low-level relative vorticity especially over the region bounded by 0°–15°N, 165°E–180° during years with RAW-warm TIO SSTAs compared to that during years with RAW-cold TIO SSTAs. Changes in vertical wind shear and low-level relative vorticity match well with the significant differences in TCs counts over the WNP basin between years with RAW-warm and RAW-cold TIO SSTAs (Fig. 3a). The increased midlevel relative humidity observed in RAW-warm TIO SSTAs relative to RAW-cold TIO SSTAs (Fig. 4c), may play a positive role in enhancing TC frequency over the WNP basin. We find no significant difference in RITCs but significant differences in TCs between years with RAW-warm and RAW-cold TIO SSTAs (Table 1) as well as changes in large-scale factors (Fig. 4). Therefore, the positive contributions to RITC counts from increased TCHP and midlevel moisture are partially cancelled by negative contributions from decreased low-level relative vorticity and increased vertical wind shear over the WNP

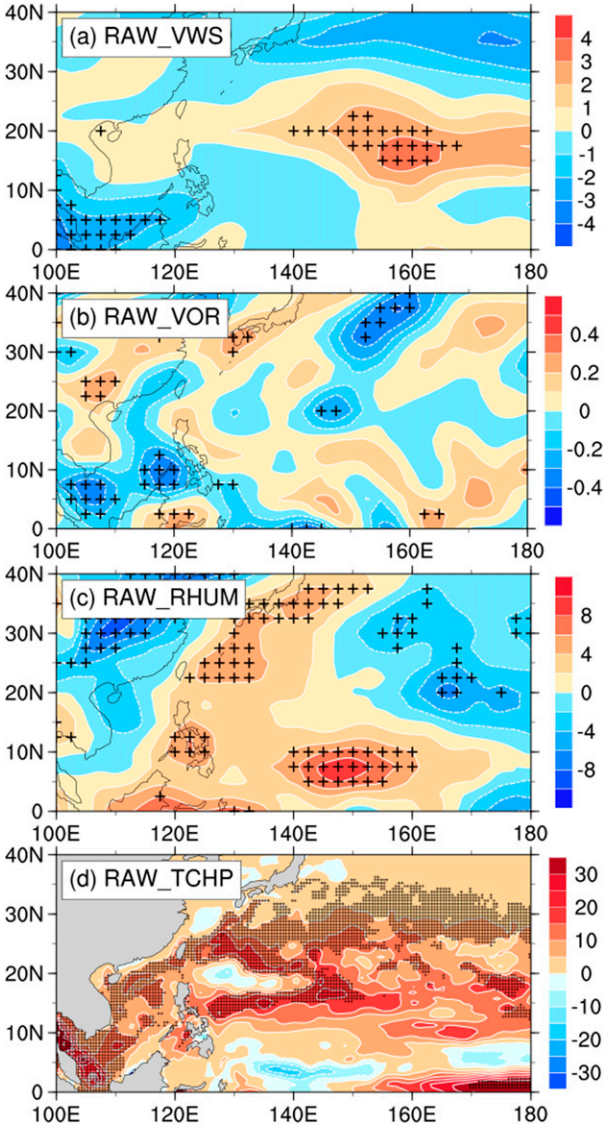

FIG. 4. Composite differences between years with warm and cold TIO SSTAs for (a) vertical wind shear ($m\,s^{-1}$), (b) 850-hPa relative vorticity ($10^{-5}\,s^{-1}$), (c) 600-hPa relative humidity (%), and (d) TCHP ($kJ\,cm^{-2}$). The plus signs (+) indicate that the differences are statistically significant between years with warm and cold TIO SSTAs at a 95% confidence level.

TABLE 1. Annually averaged RITC counts, TC counts, and the proportion of RITCs (PRITC) (%) over the WNP basin during the peak TC season (July–November) for 1979–2018, and for years with warm and cold TIO SSTAs. Statistical significance is estimated based upon a one-tailed Student's *t* test. Two asterisks (**) indicate that the difference is significant at a 95% confidence level.

	RITC	TC	PRITC
1979–2018	8.6	20	44%
Years with warm TIO SSTAs	8.6	17.8	50%
Years with cold TIO SSTAs	9	23.7	37%
Difference (warm minus cold)	−0.4	−5.9**	13%**

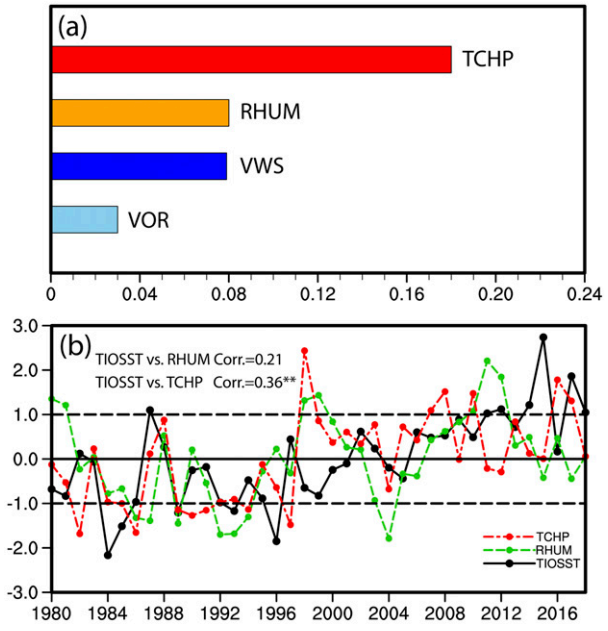

FIG. 5. (a) The absolute BDIs of large-scale environmental factors including vertical wind shear, 850-hPa relative vorticity, 600-hPa relative humidity, and TCHP between the RITC and the TC center (10° × 10°) in the main development region (7.5°–27.5°N, 110°–160°E). (b) Standardized time series of annual TIOSST (black), TCHP (red), and RHUM (green) in the main development region (7.5°–27.5°N, 110°–160°E).

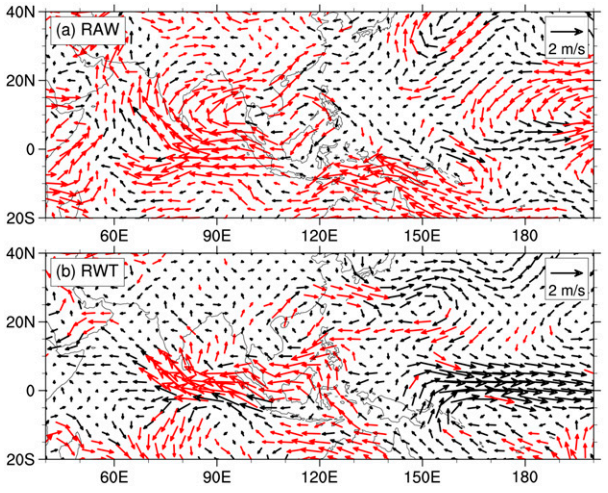

FIG. 6. (a) Composite difference of 850-hPa winds ($m\,s^{-1}$) between the years with RAW-warm and RAW-cold TIO SSTAs over July–November during 1979–2018. (b) As in (a), but between the years with RWT-warm and RWT-cold TIO SSTAs and 850-hPa winds with linear trends removed (see text for details on determining RWT-warm and RWT-cold). The red and black arrows denote 850-hPa winds, with the arrows in red being statistically significant at a 95% confidence level.

basin. Similar results have been reported in previous studies (Wang and Zhou 2008; Klotzbach 2012; Zhao et al. 2018a).

The effect of the oceanic environment (e.g., TCHP) appears to play a dominant role in controlling RITCs when compared with the atmospheric environment, similar to what has been suggested in previous studies (Wada and Chan 2008; Wang et al. 2015; C. Wang et al. 2017; Guo and Tan 2018; Zhao et al. 2018a). As shown in Fig. 4d, the difference in TCHP between years with RAW-warm and RAW-cold TIO SSTAs shows a considerable increase over the WNP basin in RAW-warm TIO SSTA years, especially over 8°–30°N, agreeing well with the main development region for RITC (15°–30°N, 120°–150°E). The close association between changes in TCHP over the WNP basin and interannual changes in TIO SSTAs is further confirmed by a significant correlation (~0.41) between TCHP over the main development region for WNP RITC and TIO SSTAs over the core region.

To further differentiate the relative importance of these four environmental factors for both TCs and RITCs, we applied the box difference index (BDI) proposed by Fu et al. (2012) and Peng et al. (2012) to rank the importance of environmental parameters differentiating RITC and TC cases by accounting for the mean and variability of the individual sample. The BDI is applied to identify controlling factors measuring the differences subjectively and quantitatively between RITC and TC cases over the MDR. Over the MDR, the RITC count is 311 (i.e., 89% of the total RITC counts), and the TC count is 689 (i.e., 86% of the total TC count). The magnitude of the BDI measures how well the variable can differentiate between rapid intensification and TC genesis. As shown in Fig. 5a, the TCHP is the most important factor contributing to RITCs, with 600-hPa relative humidity and vertical wind shear being of secondary importance. Low-level vorticity appears to only play a small role.

The greater importance of TCHP relative to midlevel moisture associated with TIO SSTA is further confirmed by both parameter's individual associations with TIO SSTAs. There is a significant correlation between TIO SST and TCHP (~0.36), while the correlation between TIO SST and midlevel relative humidity is insignificant (~0.21) (Fig. 5b). In summary, TIO SSTAs exert a significant impact on the total WNP TC number, mainly through associated changes in the dynamic factors (e.g., vertical wind shear and low-level vorticity), but RITCs are primarily modulated by associated changes of thermodynamic factors (e.g., TCHP and midlevel relative humidity).

Figure 6a shows the difference in 850-hPa winds between years with RAW-warm and RAW-cold TIO SSTAs. The increase of TCHP over the WNP basin is likely due to a positive contribution from anticyclonic circulation anomalies over the tropical Indo-Pacific regions, while the contribution of low-level westerly anomalies over the eastern portion of the tropical WNP basin likely partly cancels this positive contribution. The anticyclonic circulation anomalies over the tropical Indo-Pacific region contribute thermal energy from the atmosphere to the ocean, increasing SST and TCHP over the WNP basin (Xie et al. 2009; Liu et al. 2016). The increase in TCHP would be partly offset by increased equatorial westerly wind anomalies over the eastern portion of the WNP basin that tend

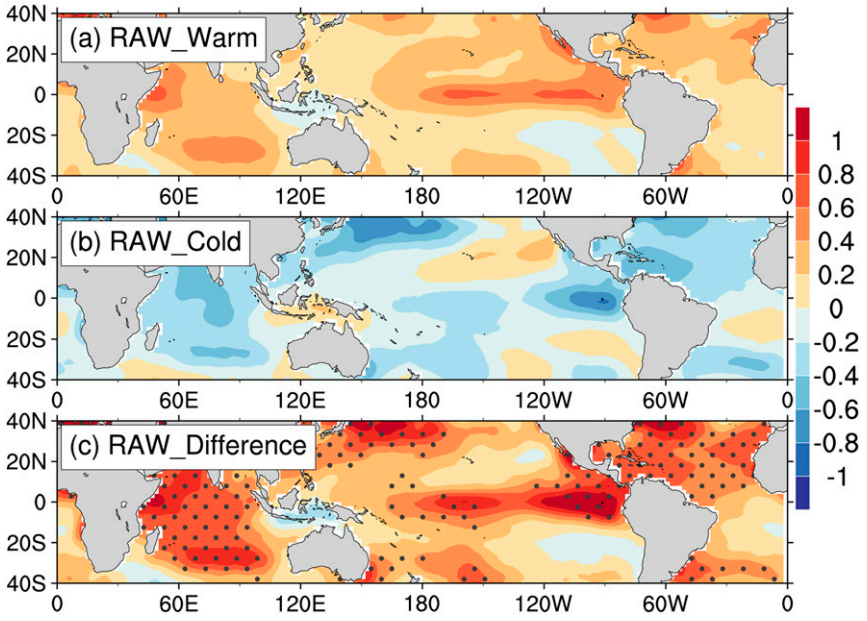

FIG. 7. Composite SST anomaly (°C) fields for (a) years with warm TIO SSTAs and (b) cold TIO SSTAs. (c) Composite differences of SST (°C) between years with warm and cold TIO SSTAs. The black dots in (c) indicate that the difference is statistically significant at a 95% confidence level.

to move warmer water toward the tropical eastern Pacific (Wang et al. 2015; Zhao and Wang 2016, 2019).

In summary, although there are significantly more TCs over the WNP basin during years with RAW-cold TIO SSTAs compared to years with RAW-warm TIO SSTAs, there is a reduced efficiency in their intensification. The lower efficiency of a TC developing into a RITC during years with RAW-cold TIO SSTAs is found to be primarily determined by decreased TCHP over the WNP basin, with an increase in RITC efficiency when RAW-warm TIO SSTAs and associated increased TCHP over the WNP basin are present. Correspondingly, an increase in PRITC over the WNP basin is observed during years with RAW-warm TIO SSTAs.

5. Possible amplification impact of global warming on WNP PRITC

Changes in oceanic and atmospheric factors are closely associated with changes in SSTAs between years with RAW-warm and RAW-cold TIO SSTAs (Fig. 7). As shown in Fig. 7c, the composite difference of SSTs between RAW-warm and RAW-cold TIO SSTAs is characterized by a tropics-wide warming, signaling the possible impact of global warming on RITC over the WNP basin. The possible impact of global warming is partly related to the fact that the selected years with RAW-warm TIO SSTAs mostly occurred during the second subperiod of 1998–2018 characterized by warmer SSTs. In fact, the upward trend in SST (0.06°C yr^{-1}) during 1979–2018 over the TIO is one of the most significant in any ocean basin around the world, as has also been indicated in previous studies (Hu and Fedorov 2019; Dong and Zhou 2014; Alory et al. 2007; Levitus et al. 2000). Additionally, prior studies have suggested a consistency between interdecadal changes in TC activity and accompanying environmental factors over the tropical WNP basin (Maue 2011; Liu and Chan 2013). Also, global warming has been implicated to possibly amplify changes in these large-scale factors (Vecchi and Soden 2007; Trenberth 2005; Knutson et al. 2010; Yang et al. 2018). The recent westward shift of the tropical upper-tropospheric trough since the late 1990s has weakened the intensity of the monsoon trough and has thus led to anomalously strong vertical wind shear and an anomalous reduction in low-level vorticity over the eastern WNP basin (Liu and Chan 2013; Hsu et al. 2014; He et al. 2017; Hu et al. 2018; Zhao et al. 2019). These findings agree well with the recent apparent decrease of TC genesis frequency over the WNP basin. A question therefore naturally arises: Is global warming amplifying the impact of interannual variability of TIO SSTAs on RITC and PRITC over the WNP basin?

To further show the possible relationship between global warming and PRITC over the WNP basin associated with interannual changes in TIO SSTAs, we first compare the standardized time series of GMSST and PRITC over the WNP basin and TIO SSTAs during JASON from 1979 to 2018 (Fig. 8). As expected, there is a significant correlation (~0.45) between WNP PRITC and GMSST during 1979–2018. The GMSST during 1979–2018 is found to be significantly associated with TIO SSTAs over the core region (30°S–20°N, 45°–90°E) ($r = 0.78$). Together with a significant increasing trend in GMSST (0.08°C yr^{-1}, significant at a 95% confidence level), these results suggest that a possible impact of global warming may be a substantial decrease in TC counts but an increased chance for RITCs and thus an increased PRITC over the WNP

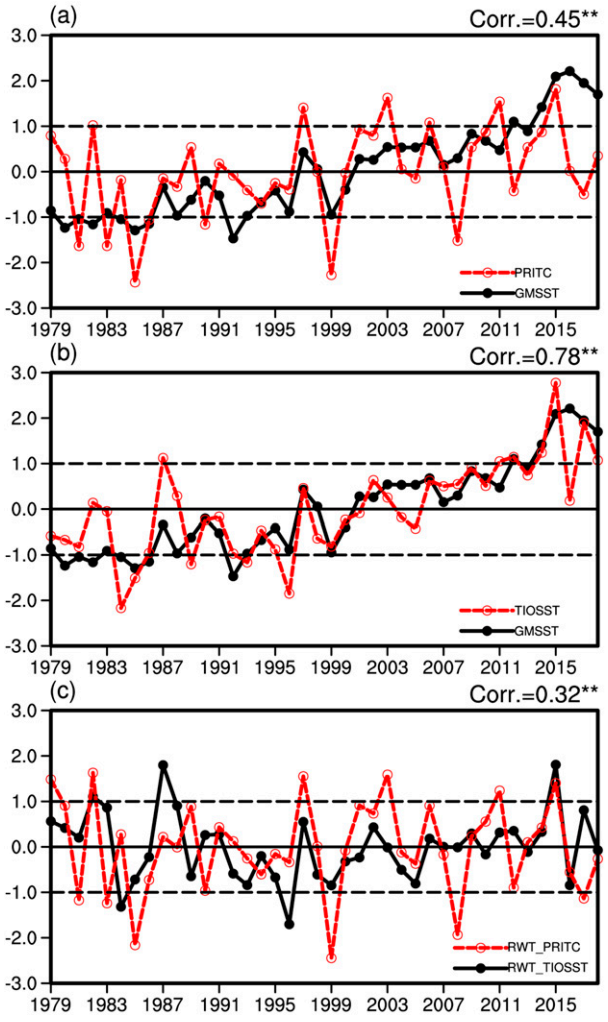

FIG. 8. Standardized time series of (a) annual WNP PRITC (red) and GMSST (black), (b) annual TIOSST (red) and GMSST index (black), and (c) annual WNP PRITC (red) and TIOSST index (black) with the linear trend removed. Two asterisks (**) indicate that the correlation is significant at a 95% confidence level.

basin in response to interannual variability in TIO SSTAs. To isolate the possible role of global warming on RITCs and PRITC over the WNP basin, we remove the associated impact of global warming on PRITC over the WNP basin by removing the linear trend of all variables. The years that we select for warm RWT-TIO SSTAs are 1982, 1983, 1987, 1988, 2015, and 2017 and the six years that we select with cold RWT-TIO SSTAs are 1984, 1993, 1996, 1999, 2005, and 2016. Other variables including TC counts, RITC counts, and PRITC over the WNP basin as well as local atmospheric and oceanic factors included in the following composite analyses between years with RWT-warm and RWT-cold TIO SSTAs are also displayed with linear trends removed.

As shown in Table 2, on average, there are ~19.0 and ~22.7 TCs during the WNP peak season, with RWT-warm and RWT-cold TIO SSTAs, respectively. The difference of 3.7 TCs is significant between years with RWT-warm and RWT-cold TIO SSTAs, but this difference is also smaller than the difference of 5.9 TCs between years with RAW-warm and RAW-cold TIO SSTAs. Similarly, the difference of RITC counts (~0.3) between years with RWT-warm and RWT-cold TIO SSTAs is not significant and is similar to the insignificant difference of RITC counts (~0.4) between years with RAW-warm and RAW-cold TIO SSTAs. Correspondingly, on an annual-average basis, there is a larger PRITC (45%) over the WNP basin during years with RWT-warm TIO SSTAs than during years with RWT-cold TIO SSTAs (37%). The difference in PRITC rate (8%) is not significant during years with RWT-warm and RWT-cold TIO SSTAs and is substantially smaller than the difference of PRITC (13%) between years with RAW-warm and RAW-cold TIO SSTAs. Moreover, the correlation of 0.46 between RAW-TIO SSTAs and PRITC over the WNP basin is reduced to 0.32 between PRITC over the WNP basin and RWT-TIO SSTAs (Figs. 2c and 8c). In summary, global warming appears to significantly reduce TCs over the WNP basin but insignificantly modulate RITCs, leading to an amplified difference of PRITC over the WNP basin between years with RAW-warm and RAW-cold TIO SSTAs.

Figure 9 shows composite SSTAs for years with RWT-warm and RWT-cold TIO SSTAs (Figs. 9a,b) as well as the differences between RWT-warm and RWT-cold years (Fig. 9c). The spatial pattern of the differences in SST between years with RWT-warm and RWT-cold TIO SSTAs is characterized by an El Niño–like pattern, with cooling SSTA over the WNP basin and a significant warming over the TIO. There is also a mostly nonsignificant warming over the tropical eastern-central Pacific in RWT-warm relative to RWT-cold TIO SSTA years (Fig. 9c). The response to such an El Niño–like pattern, in terms of the composite differences of vertical wind shear, 850-hPa relative vorticity, 600-hPa relative humidity, and TCHP over the WNP basin between years with RWT-warm and RWT-cold TIO SSTAs, is shown in Fig. 10. A decrease in vertical wind shear (Fig. 10a) over the zonal band from 10°–20°N and an increase in vertical wind shear at lower latitudes over the southeastern part of WNP basin is observed. A decrease in 850-hPa relative vorticity (Fig. 10b), especially over the main TC development region, coincides well with anticyclonic circulation anomalies (Fig. 6b). These anomalies inhibit TC development over the WNP basin during years with RWT-warm TIO SSTAs. Note that the differences in these large-scale factors between years with RWT-warm and RWT-cold TIO SSTAs are substantially smaller than those between years with RAW-warm and RAW-cold TIO SSTAs (Fig. 11). Together with the greater importance of dynamic factors (e.g., vertical wind shear and low-level relative vorticity) for TC formation and the greater importance of thermodynamic factors (e.g., TCHP and midlevel moisture) on RITC development, these results suggest that global warming may enhance the impact of large-scale environmental conditions both in reducing TC frequency and increasing the efficiency of TCs undergoing rapid intensification. Consequently, this leads to enhanced PRITC over the WNP basin during years with RAW-warm

TABLE 2. Annually averaged RITC counts, TC counts, and the proportion of RITCs (PRITC) (%) over the WNP basin during the peak TC season (July–November) after removing their linear trend for 1979–2018, and for years with warm and cold TIO SSTAs. The years with warm and cold SSTAs are selected in terms of the detrended TIO SSTA time series (labeled as years with RWT-warm and RWT-cold TIO SSTAs). Statistical significance is estimated based upon a one-tailed Student's *t* test. Two asterisks (**) indicate that the difference is significant at a 95% confidence level.

	Detrended RITC counts	Detrended TC counts	Detrended PRITC
1979–2018	8.6	20	44%
Years with RWT-warm TIO SSTAs	8.4	19	45%
Years with RWT-cold TIO SSTAs	8.7	22.7	37%
Difference (RWT-warm minus RWT-cold)	−0.3	−3.7**	8%

TIO SSTAs compared to that during years with RAW-cold TIO SSTAs.

6. Summary

In this study, we explore the interannual association between TIO SSTAs and PRITC over the WNP basin during the peak TC season (July–November) from 1979 to 2018. In agreement with previous studies on the importance of TIO SSTAs on WNP TC frequency (Du et al. 2011; Zhan et al. 2011a,b, 2014; Zhao et al. 2015), this study finds a significant negative correlation ($r = -0.44$) between TIO SSTAs and TC counts over the WNP basin. In contrast, there is a weak correlation between TIO SSTAs and RITC counts over the WNP basin. Associated with changes in TC counts and RITC counts, there is a strong interannual relationship between TIO SSTAs and PRITC over the WNP basin ($r = 0.46$). We find that there are distinct environmental factors that affect TC counts, RITC counts, and combined changes of TC counts and RITC counts (i.e., PRITC) over the WNP basin.

Other large-scale factors affecting TC and RITC counts are analyzed by exploring composite differences in TC and RITC counts over the WNP basin between years where the TIO is at least one standard deviation warmer or colder than normal (e.g., RAW-warm and RAW-cold). Significantly more TCs are observed over the WNP basin during years with RAW-cold TIO SSTAs, while there is no significant difference in RITC counts over the WNP basin during years with RAW-warm versus RAW-cold TIO SSTAs. Therefore, there is a significantly higher PRITC (50%) over the WNP basin during years with RAW-warm TIO SSTAs than the PRITC (37%) rate during years with RAW-cold TIO SSTAs. The higher PRITC rate is related to increased vertical wind shear and decreased low-level vorticity over the WNP basin (unfavorable for TC genesis during years with RAW-warm TIO SSTAs), and to

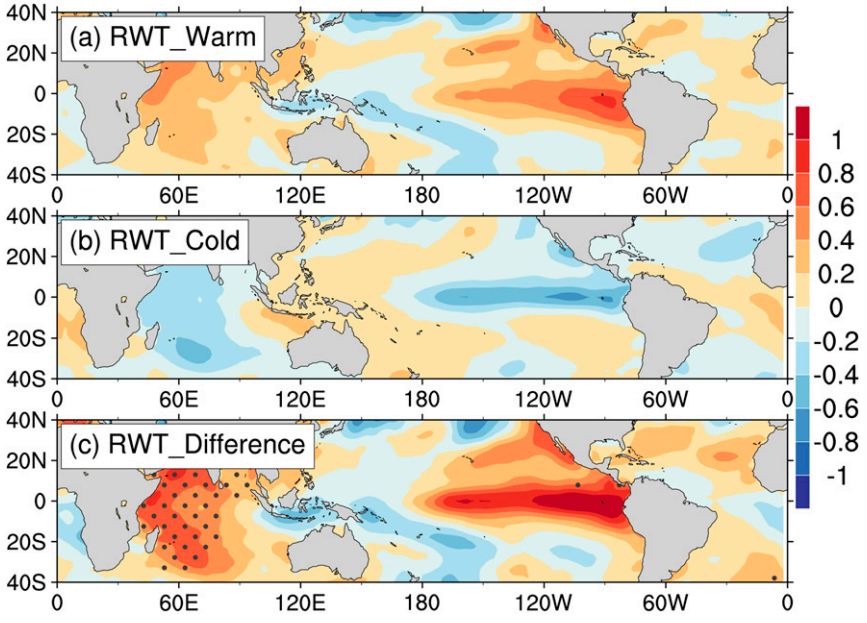

FIG. 9. Composite SST anomaly (°C) for (a) years with RWT-warm and (b) RWT-cold TIO SSTAs, as well as (c) the difference between RWT-warm and RWT-cold. The values with black dots in (c) indicate areas where the difference is statistically significant at a 95% confidence level.

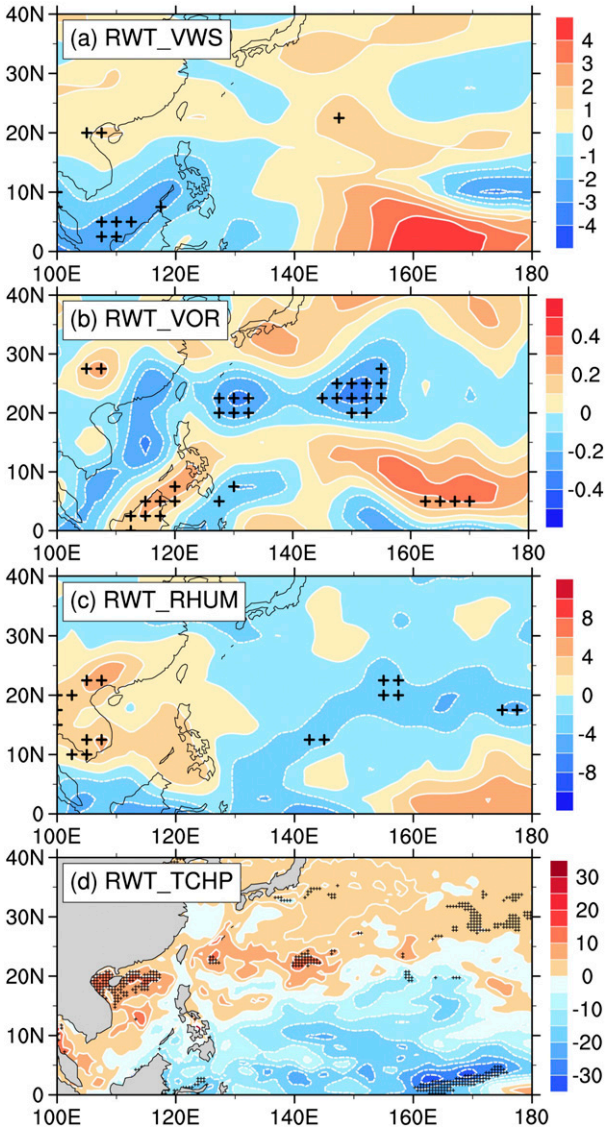

FIG. 10. Composite differences between years with RWT-warm and RWT-cold TIO SSTAs for (a) vertical wind shear ($m\,s^{-1}$), (b) 850-hPa relative vorticity ($10^{-5}\,s^{-1}$), (c) 600-hPa relative humidity (%), and (d) TCHP ($kJ\,cm^{-2}$). A plus sign (+) indicates that the differences are statistically significant between the years with RWT-warm and RWT-cold TIO SSTAs at a 95% confidence level.

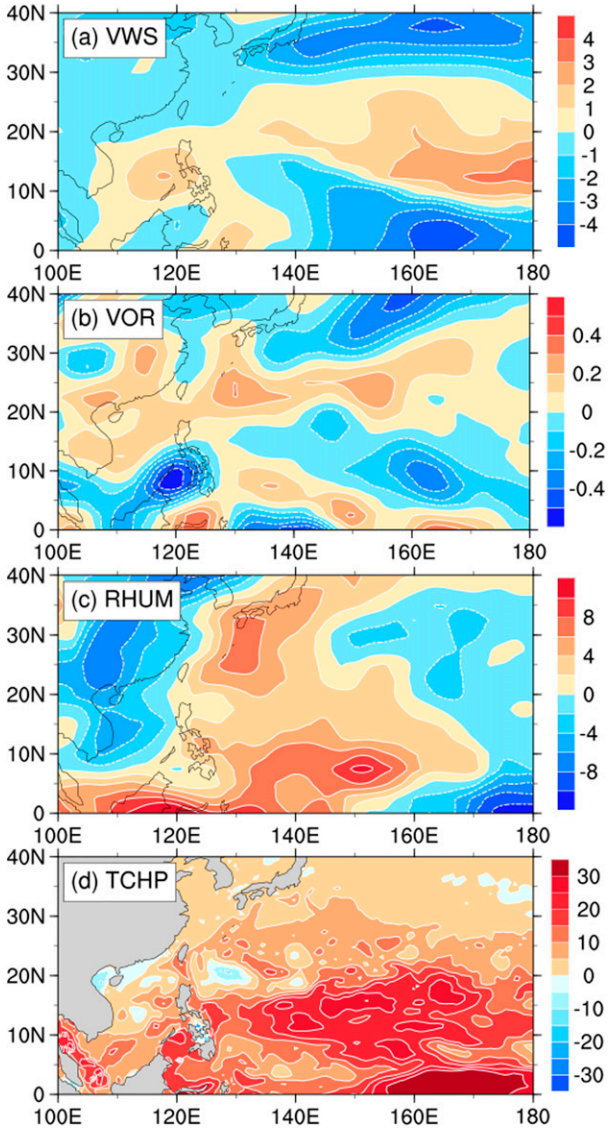

FIG. 11. Composite difference between RAW-warm and RAW-cold years and RWT-warm and RWT-cold years for (a) vertical wind shear ($m\,s^{-1}$), (b) 850-hPa relative vorticity ($10^{-5}\,s^{-1}$), (c) 600-hPa relative humidity (%), and (d) TCHP ($kJ\,cm^{-2}$).

increased TCHP and midlevel relative humidity (favorable for higher efficiency of TCs undergoing rapid intensification during years with RAW-warm TIO SSTAs). Moreover, there is also a relatively strong association between TIO SSTAs and TCHP over the WNP main development region ($r = 0.36$). The increase in TCHP over the WNP basin during years with RAW-warm TIO SSTAs is favored by an anomalous circulation over the tropical Indo-Pacific region and partly offset by anomalous low-level tropical Pacific westerlies over the eastern portion of the tropical WNP basin. Note that the substantial importance of the midlevel relative humidity for the TC rapid intensification in this study appears to be somewhat different from that in previous studies (Ma et al. 2019; Liang et al. 2018; Wu et al. 2012; Hill and Lackmann 2009). For example, Hill and Lackmann (2009) suggested that the environmental humidity is more influential for rainband activities than eyewall convection and is therefore not dominant in TC intensification. Additionally, studies (e.g., Liang et al. 2018) found that the midlevel moisture could be rather similar between rapid weakening TCs and non-rapid weakening TCs over the WMP basin, implying a limited role of environmental humidity in TC intensity change. Such inconsistency of its importance in rapid TC intensity change needs more observational analyses and numerical simulations to help us understand the

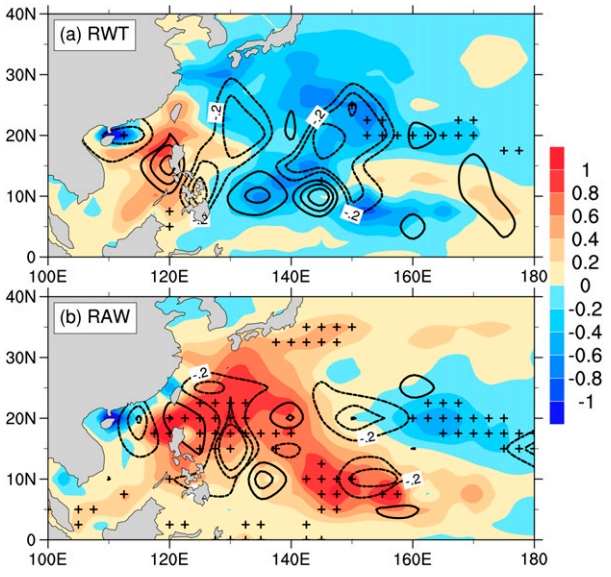

FIG. 12. (a) Composite differences in the genesis potential index (GPI) (shading) and TC genesis frequency (contour) over the WNP basin over the peak TC season during years with RWT-warm and RWT-cold TIO SSTAs. (b) As in (a), but during years with RAW-warm and RAW-cold TIO SSTAs. A plus sign (+) indicates that the differences are statistically significant between the years with RWT-warm and RWT-cold TIO SSTAs at a 95% confidence level.

climate impact of environmental humidity on TC intensity change.

A significant difference in PRITC over the WNP basin in response to the interannual variability of TIO SSTAs may be associated with the amplification impact of global warming. This potential amplification is further confirmed by examining composite differences in TC activity between years with detrended TIO SSTAs (RWT-warm versus RWT-cold TIO SSTAs). The significant difference in TC counts (~3.7) between years with RWT-warm and RWT-cold TIO SSTAs is somewhat smaller than the difference of TC counts (~5.9) between years without removing the linear trend (i.e., RAW-warm and RAW-cold TIO SSTAs). In contrast, there is no significant difference in RITC counts over the WNP basin between years with RWT-warm and RWT-cold TIO SSTAs. This value is similar to the difference observed between years with RAW-warm and RAW-cold TIO SSTAs. Correspondingly, there is a smaller difference (8%) of PRITC over the WNP basin between years using the detrended time series (i.e., RWT-warm and RWT-cold TIO SSTAs) than the difference (13%) during years with RAW-warm and RAW-cold TIO SSTAs.

We also find a reduced correlation, from 0.46 for the raw time series to 0.32 using the detrended time series, between PRITC over the WNP basin and TIO SSTA (Figs. 2c and 8c). The amplitude of the differences of large-scale factors with anomalies from the detrended time series are smaller than those between years with anomalies from the raw time series (Figs. 4 and 10). As was the case with the raw TIO SST anomalies, we find that vertical wind shear and low-level relative vorticity are more important for TC formation and that thermodynamic factors are more important for TC rapid intensification. Accompanying these changes, there is a smaller difference in TC frequency and RITCs over the WNP basin between years with RWT-warm and RWT-cold TIO SSTAs. The amplitude of increased TCHP between years with RWT-warm and RWT-cold TIO SSTAs is also smaller than that between years with RAW-warm and RAW-cold TIO SSTAs. Correspondingly, weaker anticyclonic circulation anomalies and stronger low-level westerly anomalies over the eastern portion of the WNP basin are found between years with RWT-warm and RWT-cold TIO SSTAs than during years with RAW-warm and RAW-cold TIO SSTAs. All of these results imply that global warming may strengthen the anticyclonic circulation over the tropical Indo-Pacific and reduce low-level Pacific westerly anomalies over the eastern tropical WNP, in response to interannual variability of TIO SSTAs. Global warming may also amplify the positive impact of large-scale oceanic factors and provide more chance for TC rapid intensification, while the negative impact of global warming modulates other large-scale atmospheric factors that reduce WNP TC count.

Finally, the representation of GPI developed by Emanuel and Nolan (2004) in the difference of TC genesis between years with RAW-warm/RWT-warm and RAW/RWT-cold TIO SSTAs is examined (Fig. 12). This GPI index has been widely used to represent TC genesis on various time scales (Camargo et al. 2007, 2009; Du et al. 2011; Hsu et al. 2014; Zhao et al. 2015, 2016, 2018b; Zhao and Wu 2018). Note that the composite difference of GPI (RWT-warm minus RWT-cold TIO SSTAs years) in Fig. 10a shows nearly basinwide negative GPI anomalies, consistent with the significant decrease of TCs over the WNP basin between years with RWT-warm and RWT-cold TIO SSTAs (Table 2). The positive GPI anomalies found near the Philippine Sea corresponding to an increase of TCs observed in this region. Unexpectedly, the composite GPI difference without removing the linear trend (RAW-warm minus RAW-cold TIO SSTAs years) does not spatially match the observed changes in TC genesis over the WNP basin (Fig. 12b). This result leads to the hypothesis that global warming may change the interannual relationship between some large-scale factors as well as their nonlinear interactions and TC genesis over the WNP basin. We note that these findings regarding the GPI may also be due to deficiencies in the GPI at modeling interdecadal variability and long-term trends in TC genesis (Camargo et al. 2007; Gualdi et al. 2008; Caron and Jones 2008; Zhang et al. 2010) We intend to investigate potential improvements to the GPI in future research.

Acknowledgments. This research was jointly supported by the National Natural Science Foundation of China (Grant 41922033), the Natural Science Foundation of Jiangsu Province (Grants BK20170941, BK20181412), National Natural Science Foundation of China (Grants 41675072, 41730961), the QingLan Project of Jiangsu Province (R2017Q01), the Six Talent Peaks project in Jiangsu Province (JY-100), the Postgraduate Research and Practice Innovation Program of Jiangsu Province (SJKY19_0959), and the project of Key Laboratory of South China Sea Meteorological

Disaster Prevention and Mitigation of Hainan Province, Haikou, China (SCSF201803). P. Klotzbach would like to acknowledge a grant from the G. Unger Vetlesen Foundation.

REFERENCES

Alory, G., S. Wijffels, and G. Meyers, 2007: Observed temperature trends in the Indian Ocean over 1960–1999 and associated mechanisms. *Geophys. Res. Lett.*, **34**, L02606, https://doi.org/10.1029/2006GL028044.

Bister, M., and K. A. Emanuel, 2002: Low frequency variability of tropical cyclone potential intensity 1. Interannual to interdecadal variability. *J. Geophys. Res.*, **107**, 4801, https://doi.org/10.1029/2001JD000776.

Camargo, S. J., K. A. Emanuel, and A. H. Sobel, 2007: Use of a genesis potential index to diagnose ENSO effects on tropical cyclone genesis. *J. Climate*, **20**, 4819–4834, https://doi.org/10.1175/JCLI4282.1.

——, M. C. Wheeler, and A. H. Sobel, 2009: Diagnosis of the MJO modulation of tropical cyclogenesis using an empirical index. *J. Atmos. Sci.*, **66**, 3061–3074, https://doi.org/10.1175/2009JAS3101.1.

Cao, X., S. Chen, G. Chen, and R. Wu, 2016: Intensified impact of northern tropical Atlantic SST on tropical cyclogenesis frequency over the western North Pacific after the late 1980s. *Adv. Atmos. Sci.*, **33**, 919–930, https://doi.org/10.1007/s00376-016-5206-z.

Caron, L.-P., and C. G. Jones, 2008: Analysing present, past and future tropical cyclone activity as inferred from an ensemble of coupled global climate models. *Tellus*, **60A**, 80–96, https://doi.org/10.1111/j.1600-0870.2007.00291.x.

Carton, J. A., G. A. Chepurin, and L. Chen, 2018: SODA3: A new ocean climate reanalysis. *J. Climate*, **31**, 6967–6983, https://doi.org/10.1175/JCLI-D-18-0149.1.

Chan, J. C. L., 2005: Interannual and interdecadal variations of tropical cyclone activity over the western North Pacific. *Meteor. Atmos. Phys.*, **89**, 143–152, https://doi.org/10.1007/s00703-005-0126-y.

Chu, J.-H., C. R. Sampson, A. S. Levine, and E. Fukada, 2002: The Joint Typhoon Warning Center tropical cyclone best-tracks, 1945–2000. Ref. NRL/MR/7540-02, 16 pp.

DeMaria, M., M. Mainelli, L. K. Shay, J. A. Knaff, and J. Kaplan, 2005: Further improvements to the Statistical Hurricane Intensity Prediction Scheme (SHIPS). *Wea. Forecasting*, **20**, 531–543, https://doi.org/10.1175/WAF862.1.

——, C. R. Sampson, J. A. Knaff, and K. D. Musgrave, 2014: Is tropical cyclone intensity guidance improving? *Bull. Amer. Meteor. Soc.*, **95**, 387–398, https://doi.org/10.1175/BAMS-D-12-00240.1.

Dong, L., and T. Zhou, 2014: The Indian Ocean sea surface temperature warming simulated by CMIP5 models during the twentieth century: Competing forcing roles of GHGs and anthropogenic aerosols. *J. Climate*, **27**, 3348–3362, https://doi.org/10.1175/JCLI-D-13-00396.1.

Du, Y., and S.-P. Xie, 2008: Role of atmospheric adjustments in the tropical Indian Ocean warming during the 20th century in climate models. *Geophys. Res. Lett.*, **35**, L08712, https://doi.org/10.1029/2008GL033631.

——, L. Yang, and S.-P. Xie, 2011: Tropical Indian Ocean influence on northwest Pacific tropical cyclones in summer following strong El Niño. *J. Climate*, **24**, 315–322, https://doi.org/10.1175/2010JCLI3890.1.

Elsberry, R. L., T. D. B. Lambert, and M. A. Boothe, 2007: Accuracy of Atlantic and eastern North Pacific tropical cyclone intensity forecast guidance. *Wea. Forecasting*, **22**, 747–762, https://doi.org/10.1175/WAF1015.1.

Emanuel, K., 1986: An air–sea interaction theory for tropical cyclones. Part I: Steady-state maintenance. *J. Atmos. Sci.*, **43**, 585–605, https://doi.org/10.1175/1520-0469(1986)043<0585:AASITF>2.0.CO;2.

——, 1988: The maximum intensity of hurricanes. *J. Atmos. Sci.*, **45**, 1143–1155, https://doi.org/10.1175/1520-0469(1988)045<1143:TMIOH>2.0.CO;2.

——, 1995: Sensitivity of tropical cyclones to surface exchange coefficients and a revised steady-state model incorporating eye dynamics. *J. Atmos. Sci.*, **52**, 3969–3976, https://doi.org/10.1175/1520-0469(1995)052<3969:SOTCTS>2.0.CO;2.

——, 1999: Thermodynamic control of hurricane intensity. *Nature*, **401**, 665–669, https://doi.org/10.1038/44326.

——, 2000: A statistical analysis of tropical cyclone intensity. *Mon. Wea. Rev.*, **128**, 1139–1152, https://doi.org/10.1175/1520-0493(2000)128<1139:ASAOTC>2.0.CO;2.

——, 2017: Will global warming make hurricane forecasting more difficult? *Bull. Amer. Meteor. Soc.*, **98**, 495–501, https://doi.org/10.1175/BAMS-D-16-0134.1.

——, and D. S. Nolan, 2004: Tropical cyclone activity and the global climate system. *26th Conf. on Hurricanes and Tropical Meteorology*, Miami, FL, Amer. Meteor. Soc., 240–241.

England, M. H., and Coauthors, 2014: Recent intensification of wind-driven circulation in the Pacific and the ongoing warming hiatus. *Nat. Climate Change*, **4**, 222–227, https://doi.org/10.1038/nclimate2106.

Fu, B., M. S. Peng, T. Li, and D. E. Stevens, 2012: Developing versus nondeveloping disturbances for tropical cyclone formation. Part II: Western North Pacific. *Mon. Wea. Rev.*, **140**, 1067–1080, https://doi.org/10.1175/2011MWR3618.1.

Fudeyasu, H., K. Ito, and Y. Miyamoto, 2018: Characteristics of tropical cyclone rapid intensification over the western North Pacific. *J. Climate*, **31**, 8917–8930, https://doi.org/10.1175/JCLI-D-17-0653.1.

Gelaro, R., and Coauthors, 2017: The Modern-Era Retrospective Analysis for Research and Applications, version 2 (MERRA-2). *J. Climate*, **30**, 5419–5454, https://doi.org/10.1175/JCLI-D-16-0758.1.

Goni, G. J., and J. A. Trinanes, 2003: Ocean thermal structure monitoring could aid in the intensity forecast of tropical cyclones. *Eos, Trans. Amer. Geophys. Union*, **84**, 573, https://doi.org/10.1029/2003EO510001.

——, and Coauthors, 2009: Applications of satellite-derived ocean measurements to tropical cyclone intensity forecasting. *Oceanography*, **22**, 190–197, https://doi.org/10.5670/oceanog.2009.78.

Gualdi, S., E. Scoccimarro, and A. Navarra, 2008: Changes in tropical cyclone activity due to global warming: Results from a high-resolution coupled general circulation model. *J. Climate*, **21**, 5204–5228, https://doi.org/10.1175/2008JCLI1921.1.

Guo, Y.-P., and Z.-M. Tan, 2018: Westward migration of tropical cyclone rapid-intensification over the northwestern Pacific during short duration El Niño. *Nat. Commun.*, **9**, 1507, https://doi.org/10.1038/s41467-018-03945-y.

He, H. Z., J. Yang, L. G. Wu, D. Y. Gong, B. Wang, and M. N. Gao, 2017: Unusual growth in intense typhoon occurrences over the Philippine Sea in September after the mid-2000s. *Climate Dyn.*, **48**, 1893–1910, https://doi.org/10.1007/s00382-016-3181-9.

Hill, K. A., and G. M. Lackmann, 2009: Influence of environmental humidity on tropical cyclone size. *Mon. Wea. Rev.*, **137**, 3294–3315, https://doi.org/10.1175/2009MWR2679.1.

Hoerling, M. P., J. W. Hurrell, T. Xu, G. T. Bates, and A. S. Phillips, 2004: Twentieth century North Atlantic climate change. Part II: Understanding the effect of Indian Ocean warming. *Climate Dyn.*, **23**, 391–405, https://doi.org/10.1007/s00382-004-0433-x.

Hsu, P.-C., P.-S. Chu, H. Murakami, and X. Zhao, 2014: An abrupt decrease in the late-season typhoon activity over the western North Pacific. *J. Climate*, **27**, 4296–4312, https://doi.org/10.1175/JCLI-D-13-00417.1.

Hu, A., and S. C. Bates, 2018: Internal climate variability and projected future regional steric and dynamic sea level rise. *Nat. Commun.*, **9**, 1068, https://doi.org/10.1038/s41467-018-03474-8.

Hu, C., C. Zhang, S. Yang, D. Chen, and S. He, 2018: Perspective on the northwestward shift of autumn tropical cyclogenesis locations over the western North Pacific from shifting ENSO. *Climate Dyn.*, **51**, 2455–2465, https://doi.org/10.1007/s00382-017-4022-1.

Hu, K., G. Huang, X.-T. Zheng, S.-P. Xie, X. Qu, Y. Du, and L. Liu, 2014: Interdecadal variations in ENSO influences on northwest Pacific–East Asian early summertime climate simulated in CMIP5 models. *J. Climate*, **27**, 5982–5998, https://doi.org/10.1175/JCLI-D-13-00268.1.

Hu, S., and A. V. Fedorov, 2019: Indian Ocean warming can strengthen the Atlantic meridional overturning circulation. *Nat. Climate Change*, **9**, 747–751, https://doi.org/10.1038/s41558-019-0566-x.

Huang, B., and Coauthors, 2017: Extended Reconstructed Sea Surface Temperature, version 5 (ERSSTv5): Upgrades, validations, and intercomparisons. *J. Climate*, **30**, 8179–8205, https://doi.org/10.1175/JCLI-D-16-0836.1.

Huo, L., P. Guo, S. N. Hameed, and D. Jin, 2015: The role of tropical Atlantic SST anomalies in modulating western North Pacific tropical cyclone genesis. *Geophys. Res. Lett.*, **42**, 2378–2384, https://doi.org/10.1002/2015GL063184.

Ihara, C., Y. Kushnir, M. A. Cane, and V. H. de la Peña, 2009: Climate change over the equatorial Indo-Pacific in global warming. *J. Climate*, **22**, 2678–2693, https://doi.org/10.1175/2008JCLI2581.1.

Kanamitsu, M., W. Ebisuzaki, J. Woollen, S.-K. Yang, J. J. Hnilo, M. Fiorino, and G. L. Potter, 2002: NCEP–DOE AMIP-II Reanalysis (R-2). *Bull. Amer. Meteor. Soc.*, **83**, 1631–1643, https://doi.org/10.1175/BAMS-83-11-1631.

Kang, N.-Y., and J. B. Elsner, 2019: Influence of global warming on the rapid intensification of western North Pacific tropical cyclones. *Environ. Res. Lett.*, **14**, 44027, https://doi.org/10.1088/1748-9326/ab0b50.

Kaplan, J., and M. DeMaria, 2003: Large-scale characteristics of rapidly intensifying tropical cyclones in the North Atlantic basin. *Wea. Forecasting*, **18**, 1093–1108, https://doi.org/10.1175/1520-0434(2003)018<1093:LCORIT>2.0.CO;2.

Klotzbach, P. J., 2012: El Niño–Southern Oscillation, the Madden–Julian Oscillation and Atlantic basin tropical cyclone rapid intensification. *J. Geophys. Res.*, **117**, D14104, https://doi.org/10.1029/2012JD017714.

Knutson, T. R., and Coauthors, 2010: Tropical cyclones and climate change. *Nat. Geosci.*, **3**, 157–163, https://doi.org/10.1038/ngeo779.

Leipper, D. F., 1967: Observed ocean conditions and Hurricane Hilda, 1964. *J. Atmos. Sci.*, **24**, 182–186, https://doi.org/10.1175/1520-0469(1967)024<0182:OOCAHH>2.0.CO;2.

——, and D. Volgenau, 1972: Hurricane heat potential of the Gulf of Mexico. *J. Phys. Oceanogr.*, **2**, 218–224, https://doi.org/10.1175/1520-0485(1972)002<0218:HHPOTG>2.0.CO;2.

Levitus, S., J. I. Antonov, T. P. Boyer, and C. Stephens, 2000: Warming of the world ocean. *Science*, **287**, 2225–2229, https://doi.org/10.1126/science.287.5461.2225.

Liang, J., L. Wu, and G. Gu, 2018: Rapid weakening of tropical cyclones in monsoon gyres over the tropical western North Pacific. *J. Climate*, **31**, 1015–1028, https://doi.org/10.1175/JCLI-D-16-0784.1.

Lin, I.-I., C.-C. Wu, K. A. Emanuel, I.-H. Lee, C.-R. Wu, and I.-F. Pun, 2005: The interaction of Supertyphoon Maemi (2003) with a warm ocean eddy. *Mon. Wea. Rev.*, **133**, 2635–2649, https://doi.org/10.1175/MWR3005.1.

——, ——, I.-F. Pun, and D.-S. Ko, 2008: Upper-ocean thermal structure and the western North Pacific category 5 typhoons. Part I: Ocean features and the category 5 typhoons' intensification. *Mon. Wea. Rev.*, **136**, 3288–3306, https://doi.org/10.1175/2008MWR2277.1.

——, I. Pun, and C. Lien, 2014: "Category-6" supertyphoon Haiyan in global warming hiatus: Contribution from subsurface ocean warming. *Geophys. Res. Lett.*, **41**, 8547–8553, https://doi.org/10.1002/2014GL061281.

Liu, K. S., and J. C. L. Chan, 2013: Inactive period of western North Pacific tropical cyclone activity in 1998–2011. *J. Climate*, **26**, 2614–2630, https://doi.org/10.1175/JCLI-D-12-00053.1.

Liu, R., C. Chen, and G. Wang, 2016: Change of tropical cyclone heat potential in response to global warming. *Adv. Atmos. Sci.*, **33**, 504–510, https://doi.org/10.1007/s00376-015-5112-9.

Luo, J. J., W. Sasaki, and Y. Masumoto, 2012: Indian Ocean warming modulates Pacific climate change. *Proc. Natl. Acad. Sci. USA*, **109**, 18 701–18 706, https://doi.org/10.1073/pnas.1210239109.

Ma, Z., J. Fei, L. Liu X. Huang, and Y. Li, 2017: An investigation of the influences of mesoscale ocean eddies on tropical cyclone intensities. *Mon. Wea. Rev.*, **145**, 1181–1201, https://doi.org/10.1175/MWR-D-16-0253.1.

——, ——, and X. Huang, 2019: A definition of rapid weakening for tropical cyclones over the western North Pacific. *Geophys. Res. Lett.*, **46**, 11 471–11 478, https://doi.org/10.1029/2019GL085090.

Mainelli, M., M. DeMaria, L. K. Shay, and G. Goni, 2008: Application of oceanic heat content estimation to operational forecasting of recent Atlantic category 5 hurricanes. *Wea. Forecasting*, **23**, 3–16, https://doi.org/10.1175/2007WAF2006111.1.

Maue, R. N., 2011: Recent historically low global tropical cyclone activity. *Geophys. Res. Lett.*, **38**, L14803, https://doi.org/10.1029/2011GL047711.

Mendelsohn, R., K. Emanuel, S. Chonabayashi, and L. Bakkensen, 2012: The impact of climate change on global tropical cyclone damage. *Nat. Climate Change*, **2**, 205–209, https://doi.org/10.1038/nclimate1357.

Peduzzi, P., B. Chatenoux, H. Dao, A. De Bono, C. Herold, J. Kossin, F. Mouton, and O. Nordbeck, 2012: Global trends in tropical cyclone risk. *Nat. Climate Change*, **2**, 289–294, https://doi.org/10.1038/nclimate1410.

Peng, M. S., B. Fu, T. Li, and D. E. Stevens, 2012: Developing versus nondeveloping disturbances for tropical cyclone formation. Part I: North Atlantic. *Mon. Wea. Rev.*, **140**, 1047–1066, https://doi.org/10.1175/2011MWR3617.1.

Rappaport, E. N., and Coauthors, 2009: Advances and challenges at the National Hurricane Center. *Wea. Forecasting*, **24**, 395–419, https://doi.org/10.1175/2008WAF2222128.1.

Roxy, M. K., K. Ritika, P. Terray, and S. Masson, 2014: The curious case of Indian Ocean warming. *J. Climate*, **27**, 8501–8509, https://doi.org/10.1175/JCLI-D-14-00471.1.

Scharroo, R., W. H. F. Smith, and J. L. Lillibridge, 2005: The intensification of Hurricane Katrina observed by satellite

altimetry. *Eos, Trans. Amer. Geophys. Union*, **86**, 366, https://doi.org/10.1029/2005EO400004.

Schreck, C. J., K. R. Knapp, and J. P. Kossin, 2014: The impact of best track discrepancies on global tropical cyclone climatologies using IBTrACS. *Mon. Wea. Rev.*, **142**, 3881–3899, https://doi.org/10.1175/MWR-D-14-00021.1.

Shay, L. K., G. J. Goni, and P. G. Black, 2000: Effects of a warm oceanic feature on Hurricane Opal. *Mon. Wea. Rev.*, **128**, 1366–1383, https://doi.org/10.1175/1520-0493(2000)128<1366:EOAWOF>2.0.CO;2.

Shi, D., X. Ge, M. Peng, and T. Li, 2020: Characterization of tropical cyclone rapid intensification under two types of El Niño events in the western North Pacific. *Int. J. Climatol.*, **40**, 2359–2372, https://doi.org/10.1002/JOC.6338.

Shu, S., J. Ming, and P. Chi, 2012: Large-scale characteristics and probability of rapidly intensifying tropical cyclones in the western North Pacific basin. *Wea. Forecasting*, **27**, 411–423, https://doi.org/10.1175/WAF-D-11-00042.1.

Tao, L., and S. C. Cheng, 2012: Impact of Indian Ocean basin warming and ENSO on tropical cyclone activities over the western Pacific. *Chin. J. Atmos. Sci.*, **36**, 1223–1235.

Tao, W., G. Huang, K. Hu X. Qu, G. Wen, and H. Gong, 2015: Interdecadal modulation of ENSO teleconnections to the Indian Ocean basin mode and their relationship under global warming in CMIP5 models. *Int. J. Climatol.*, **35**, 391–407, https://doi.org/10.1002/joc.3987.

Trenberth, K., 2005: Uncertainty in hurricanes and global warming. *Science*, **308**, 1753–1754, https://doi.org/10.1126/SCIENCE.1112551.

Vecchi, G. A., and B. J. Soden, 2007: Increased tropical Atlantic wind shear in model projections of global warming. *Geophys. Res. Lett.*, **34**, L08702, https://doi.org/10.1029/2006GL028905.

Wada, A., and J. C. L. Chan, 2008: Relationship between typhoon activity and upper ocean heat content. *Geophys. Res. Lett.*, **35**, L17603, https://doi.org/10.1029/2008GL035129.

Wang, B., and X. Zhou, 2008: Climate variation and prediction of rapid intensification in tropical cyclones in the western North Pacific. *Meteor. Atmos. Phys.*, **99** (1-2), 1–16, https://doi.org/10.1007/s00703-006-0238-z.

Wang, C., W. Wang, D. Wang, and Q. Wang, 2006: Interannual variability of the South China Sea associated with El Niño. *J. Geophys. Res.*, **111**, C03023, https://doi.org/10.1029/2005jc003333.

——, X. Wang, R. H. Weisberg, and M. L. Black, 2017: Variability of tropical cyclone rapid intensification in the North Atlantic and its relationship with climate variations. *Climate Dyn.*, **49**, 3627–3645, https://doi.org/10.1007/s00382-017-3537-9.

Wang, L., J. Y. Yu, and H. Paek, 2017: Enhanced biennial variability in the Pacific due to Atlantic capacitor effect. *Nat. Commun.*, **8**, 14887, https://doi.org/10.1038/NCOMMS14887.

Wang, X., and H. Liu, 2016: PDO modulation of ENSO effect on tropical cyclone rapid intensification in the western North Pacific. *Climate Dyn.*, **46**, 15–28, https://doi.org/10.1007/s00382-015-2563-8.

——, C. Wang, L. Zhang, and X. Wang, 2015: Multidecadal variability of tropical cyclone rapid intensification in the western North Pacific. *J. Climate*, **28**, 3806–3820, https://doi.org/10.1175/JCLI-D-14-00400.1.

Wu, L., and Coauthors, 2012: Relationship of environmental relative humidity with North Atlantic tropical cyclone intensity and intensification rate. *Geophys. Res. Lett.*, **39**, L20809, https://doi.org/10.1029/2012GL053546.

Xie, S.-P., K. Hu, J. Hafner, H. Tokinaga, Y. Du, G. Huang, and T. Sampe, 2009: Indian Ocean capacitor effect on Indo–western Pacific climate during the summer following El Niño. *J. Climate*, **22**, 730–747, https://doi.org/10.1175/2008JCLI2544.1.

——, Y. Kosaka, Y. Du, K. Hu, J. S. Chowdary, and G. Huang, 2016: Indo-western Pacific ocean capacitor and coherent climate anomalies in post-ENSO summer: A review. *Adv. Atmos. Sci.*, **33**, 411–432, https://doi.org/10.1007/s00376-015-5192-6.

Yang, S.-H., N.-Y. Kang, J. B. Elsner, and Y. Chun, 2018: Influence of global warming on western North Pacific tropical cyclone intensities during 2015. *J. Climate*, **31**, 919–925, https://doi.org/10.1175/JCLI-D-17-0143.1.

Zhan, R., Y. Wang, and X. Lei, 2011a: Contributions of ENSO and east Indian Ocean SSTA to the interannual variability of northwest Pacific tropical cyclone frequency. *J. Climate*, **24**, 509–521, https://doi.org/10.1175/2010JCLI3808.1.

——, ——, and C.-C. Wu, 2011b: Impact of SSTA in the east Indian Ocean on the frequency of northwest Pacific tropical cyclones: A regional atmospheric model study. *J. Climate*, **24**, 6227–6242, https://doi.org/10.1175/JCLI-D-10-05014.1.

——, ——, and L. Tao, 2014: Intensified impact of east Indian Ocean SST anomaly on tropical cyclone genesis frequency over the western North Pacific. *J. Climate*, **27**, 8724–8739, https://doi.org/10.1175/JCLI-D-14-00119.1.

——, B. Chen, and Y. Ding, 2018: Impacts of SST anomalies in the Indian-Pacific basin on northwest Pacific tropical cyclone activities during three super El Niño years. *J. Oceanol. Limnol.*, **36**, 20–32, https://doi.org/10.1007/s00343-018-6321-8.

Zhang, Q., L. Wu, and Q. Liu, 2009: Tropical cyclone damages in China 1983–2006. *Bull. Amer. Meteor. Soc.*, **90**, 489–496, https://doi.org/10.1175/2008BAMS2631.1.

——, W. Zhang, Y. D. Chen, and T. Jiang, 2011: Flood, drought and typhoon disasters during the last half-century in the Guangdong province, China. *Nat. Hazards*, **57**, 267–278, https://doi.org/10.1007/s11069-010-9611-9.

Zhang, Y., H. Wang, J. Sun, and H. Drange, 2010: Changes in the tropical cyclone genesis potential index over the western North Pacific in the SRES A2 scenario. *Adv. Atmos. Sci.*, **27**, 1246–1258, https://doi.org/10.1007/s00376-010-9096-1.

Zhao, H., and C. Wang, 2016: Interdecadal modulation on the relationship between ENSO and typhoon activity during the late season in the western North Pacific. *Climate Dyn.*, **47**, 315–328, https://doi.org/10.1007/s00382-015-2837-1.

——, and L. Wu, 2018: Modulation of convectively coupled equatorial Rossby wave on the western North Pacific tropical cyclones activity. *Int. J. Climatol.*, **38**, 932–948, https://doi.org/10.1002/joc.5220.

——, and C. Wang, 2019: On the relationship between ENSO and tropical cyclones in the western North Pacific during the boreal summer. *Climate Dyn.*, **52**, 275–288, https://doi.org/10.1007/s00382-018-4136-0.

——, P.-S. Chu, P.-C. Hsu, and H. Murakami, 2014: Exploratory analysis of extremely low tropical cyclone activity during the late-season of 2010 and 1998 over the western North Pacific and the South China Sea. *J. Adv. Model. Earth Syst.*, **6**, 1141–1153, https://doi.org/10.1002/2014MS000381.

——, X. Jiang, and L. Wu, 2015: Modulation of northwest Pacific tropical cyclone genesis by the intraseasonal variability. *J. Meteor. Soc. Japan*, **93**, 81–97, https://doi.org/10.2151/JMSJ.2015-006.

——, ——, and ——, 2016: Boreal summer synoptic-scale waves over the western North Pacific in multimodel simulations. *J. Climate*, **29**, 4487–4508, https://doi.org/10.1175/JCLI-D-15-0696.1.

——, X. Duan, G. B. Raga, and P. J. Klotzbach, 2018a: Changes in characteristics of rapidly intensifying western North Pacific tropical cyclones related to climate regime shifts. *J. Climate*, **31**, 8163–8179, https://doi.org/10.1175/JCLI-D-18-0029.1.

——, G. B. Raga, and P. J. Klotzbach, 2018b: Impact of the boreal summer quasi-biweekly oscillation on eastern North Pacific tropical cyclone activity. *Int. J. Climatol.*, **38**, 1353–1365, https://doi.org/10.1002/JOC.5250.

——, S. Chen, and P. J. Klotzbach, 2019: Recent strengthening of the relationship between the western North Pacific monsoon and western North Pacific tropical cyclone activity during the boreal summer. *J. Climate*, **32**, 8283–8299, https://doi.org/10.1175/JCLI-D-19-0016.1.

Zheng, X.-T., S.-P. Xie, and Q. Liu, 2011: Response of the Indian Ocean basin mode and its capacitor effect to global warming. *J. Climate*, **24**, 6146–6164, https://doi.org/10.1175/2011JCLI4169.1.

——, ——, Y. Du, L. Liu, G. Huang, and Q. Liu, 2013: Indian Ocean dipole response to global warming in the CMIP5 multimodel ensemble. *J. Climate*, **26**, 6067–6080, https://doi.org/10.1175/JCLI-D-12-00638.1.